Fatigue limit evaluation of metals using an infrared thermographic technique

Minh-Phong Luong

Fatigue limit evaluation of metals using an infrared thermographic technique

Minh Phong Luong

CNRS-LMS Ecole Polytechnique, 91128 Palaiseau, France

Abstract The paper aims to illustrate three advantages of infrared thermography as a non-destructive, real-time and non-contact technique. It permits first observation of the physical processes of damage and failure in metals, and in particular, automotive components subjected to fatigue loading, second detection of the occurrence of intrinsic dissipation, and third evaluation of the fatigue strength in a very short time, compared to traditional testing techniques. In addition, infrared thermography readily describes the damage location and the evolution of structural failure.

Keywords: Automotive components; Damage detection; Fast evaluation of fatigue limit; Infrared thermography; Intrinsic dissipation; Non-destructive testing

1. Introduction

Metal fatigue of aircraft components was detected very early in the history of powered flight (Mann, 1983), and it was also of major importance in determining the durability of ground vehicles. The failure mode was identified early by railway engineers. Vehicles and tracks are expected to last up to 40 years, and bridges 120 years. A large number of potential opportunities for fatigue failure exists. Even very low failure rates can produce an appreciable number of failures (McLester, 1988). Fatigue phenomena, leading for example to the failure of diesel engines (Habib and Husain, 1994), were poorly understood until recently because they occur unexpectedly at relatively low stress levels. Some progress has been made recently in design methods (Ballard et al., 1995). Nevertheless, these methods must be used in conjunction with reliable experimental procedures. Fatigue criteria and fracture controls are needed, together with practical and economic considerations. Thus fatigue testing is central to the process of design assessment, and is complementary to analytical and numerical methods. Traditionally, experimental methods correlate the fatigue life of a smooth specimen under uniaxial stress conditions with constant amplitude of either plastic strain or stress. Multiaxial fatigue assessment is then carried out with the help of an appropriate rule or criterion that reduces the complex multiaxial loading to an equivalent uniaxial loading. Morrow (1965) investigated the relationship among cyclic stress, plastic strain, and the fatigue damage process. Since fatigue is

* E-mail: luong@athena.polytechnique.fr.

generally caused by cyclic plastic strain, the plastic strain energy plays a very significant role in the damage process (Ellyin and Kujawski, 1984; Irwin, 1965; Mroz, 1983). Therefore, the idea of relating fatigue to the intrinsic dissipation is highly relevant.

This paper emphasises the application of infrared thermography to detect the occurrence of damage and the fatigue process in metals, and subsequently to evaluate the fatigue limit in a very short time, defined as a drastic change in the rate of intrinsic dissipation.

2. Quantitative measurement of damage

Damage theories rely on assumed discontinuous phenomena at the microscopic scale (Bui and Stolz, 1987). At the macroscopic scale, damage parameters, considered as internal variables, are introduced according to the following three main approaches.

2.1. Effective stress

Kachanov (1958) introduced a continuous variable D, related to the scalar density of defects. The elastic body is assumed to contain many cracks. Thus, the cracks increase the compliances and decrease the stiffness. This has been the starting point of damage theories developed for analysing fatigue in metals, creep, and creep-fatigue interaction.

2.2. Plasticity formalism

The plasticity formalism describes the inelastic behaviour of progressively fracturing solids by introducing the concept of fracturing stress and fracturing strain. The elastic–plastic fracturing model combines the elastic–plastic law and the elastic–brittle law. Taking into account the most fundamental aspects of inelastic deformation and neglecting the details at the microstructural level, Mroz (1986) suggests phenomenological constitutive models that are widely used in engineering applications.

2.3. Micromechanics

On the basis of micro- and macro-scale relationships, Dang-van (1973) proposed a multiaxial fatigue criterion with a realistic physical interpretation of fatigue phenomena. During a polycyclic fatigue test, the stress at the macroscopic scale remains elastic. However, at the microscopic scale, the metal is neither isotropic nor homogeneous. It is constituted of randomly oriented crystals. This induces local fluctuations of the microscopic stress and defines the macroscopic stress. Thus, the local microscopic stress can locally exceed the yield strength in certain unfavourably oriented grains, whereas the macroscopic stress remains elastic. If the cyclic plastic response of the grain is not an elastic shakedown, then some microcracks will be nucleated. They could coalesce to form a crack of detectable size. This formulation has been recently extended for a better fitting with experimental results (Deperrois, 1991).

Despite this wealth of methods developed by engineers over the years, the principal question that remains unanswered is: what is the physical phenomenon called fatigue damage? Several types of fatigue damage have been identified by Mughrabi et al. (1983) and Polak et al. (1996) without leading to a practical quantitative characterisation. Many attempts have been made to measure local plastic strains within individual grains (James and Morris, 1983; Field et al., 1983; Cabañas-Moreno et al., 1983; Baxter, 1983; Pluvinage and Raguet, 1983; Kitagawa et al., 1983; McEvily, 1983; Loye et al., 1983; Ranganathan and Petit, 1983).

The ASTM STP 811 meeting in 1982 concluded that fatigue damage can be defined as: (i) a chemical–physical process whereby irreversible degradation of a specific property results from the application of cyclic stress and strain, or (ii) a physical separation of the material (cracks, cavitation, etc.).

Understanding fatigue damage requires making a clear distinction between the physical damage, the process of damage, and the *manifestation of damage*. This experimental work is based on the assumption that intrinsic dissipation and damage present the same evolution under cyclic loading as they occur in traditional fatigue tests used for determining the endurance limit.

3. Heat production mechanism

Various heat production mechanisms have been proposed by various authors and are now discussed.

According to Moore and Kommers (1921), the temperature test was suggested and to some extent used by C.E. Stromeyer of Manchester in England as early as 1913. However, their search for some short-time test to predict fatigue resistance, based on the use of thermocouples was not conclusive since they could not identify a critical temperature with the endurance limit of steel specimens subjected to cyclic loading.

Traditionally, the question of why a crack initiates and propagates is raised. It seems to be rather philosophical when searching for short-time testing techniques to determine the fatigue limit. This paper proposes using differential infrared thermography to quantitatively evaluate the *evolution of temperature* generated by the specimen under reversed stresses applied for a few minutes or less. The infrared thermographic technique could readily detect the occurrence of both initiation and propagation of failure. It could be used to establish allowable stress levels and inspection requirements so that fracture cannot occur.

Infrared thermography has been successfully used as an experimental method to detect the plastic deformation of a steel plate under monotonic loading (Bui et al., 1981), or as a laboratory technique for investigating damage, fatigue, and failure mechanisms occurring in engineering materials (Luong, 1990). Plastic deformation is not homogeneous and the stress acting on a plastic inhomogeneity embedded in an elastic surrounding is a function of its plastic strain, diminishing with increasing strain. Due to the thermomechanical coupling, the generated plastic dissipation is readily detected by infrared thermography.

4. Infrared thermography background

The development of the thermo-elastic–plasticity equations requires three basic assumptions (Allen, 1985; Dillon, 1963; Kratochvil and Dillon, 1969; Farren and Taylor, 1925).

- The basic thermomechanical quantities describing thermodynamic processes: the motion x, the second Piola–Kirchhoff stress tensor S, the body force per unit mass b, the Helmholtz free energy ψ, the specific entropy s, the heat supply r_0, the absolute temperature T, the heat flux vector per unit area q, the elastic strain tensor E^{e}, the inelastic strain tensor E^{I}, and a set of internal state variables $\alpha^{(\mathrm{I})}$ characterising the material.
- The fundamental balance laws of linear momentum, angular momentum, and energy, as well as the second law of thermodynamics expressed in the variables given above.
- The constitutive laws describing the material response.

This leads to the following coupled thermomechanical equation:

$$\rho C_{\mathrm{v}} \dot{T} = r_0 + K \nabla^2 T - \left(\beta : \overset{4}{D} : \dot{E}^{e} \right) T + S : \dot{E}^{I}$$

where β denotes the coefficient of the thermal expansion matrix, C_{v} (J kg^{-1} K^{-1}: Joule per kilogram per kelvin) the specific heat at constant deformation, $\overset{4}{D}$ the fourth-order elasticity tensor, e the specific internal energy, K (W m^{-1} K^{-1}: Watt per metre per kelvin) the thermal conductivity, and finally, T the absolute temperature. The volumetric heat capacity $C = \rho C_{\mathrm{v}}$ of the material is the energy required to raise the temperature of a unit volume by 1°C (or kelvin).

This equation shows the potential applications of the infrared scanning technique in diverse engineering domains (detection of fluid leakages, non-destructive testing using thermal conduction phenomena, elastic stress measurements, and localisation of dissipative phenomena). The detected temperature change, resulting from four quite different phenomena, must be correctly discriminated by particular test conditions and/or specific data reduction. This is the main difficulty when interpreting the thermal images obtained from experiments under the usual conditions.

4.1. Heat sources

The first term on the right-hand side of the thermomechanical equation is due to sources or sinks of heat in the scanning field. The surface heat patterns displayed on the scanned specimen could be either established by external heating, referred to in the

literature as passive heating, and due to local differences in thermal conductivity caused by variations on isothermal patterns, or by internally generated heat referred to as active heating. In the following reported experiments, thermal noise generated by gripping systems could obscure the intrinsic dissipation generated by the specimen under test loading.

4.2. Thermal conduction

The second term on the right-hand side of the thermomechanical equation governs the transfer of heat by conduction which leads to a uniform temperature on the specimen. The variation in thermal conductivity could be caused by local inhomogeneities or flaws in the materials. If a transient flow exists, then thermal behaviour is governed not only by the thermal conductivity but also by the heat capacity. The ratio of these two properties is termed the thermal diffusivity $\alpha = K/C$ ($m^2\ s^{-1}$) that becomes the governing parameter for transient states. A high value of the thermal diffusivity implies a capability for rapid and considerable changes in temperature. It is important to bear in mind that two materials may have very dissimilar thermal conductivities. A pulsed heat flux has been used to characterise a delamination in a composite by the break cause in the temperature-time history.

4.3. Thermoelasticity

The third term on the right-hand side of the thermomechanical equation illustrates the thermoelastic coupling effect. Within the elastic range and when subjected to tensile or compressive stresses, a material experiences a reversible conversion between the mechanical and thermal energy responsible for a temperature change. Provided adiabatic conditions are maintained, the relationship between the change in the first stress invariant and the associated change in temperature is linear and independent of loading frequency. It is the reversible portion of the mechanical energy generated. A stress analysis technique known as SPATE (Stress Pattern Analysis by Thermal Emissions) measures the temperature due to the thermoelastic heating and cooling of a body under cyclic loading (Oliver, 1986).

4.4. Intrinsic dissipation

The last term on the right-hand side of the thermomechanical equation defines the energy dissipation due to plasticity and/or viscosity. Its has been recognised by many scientists (Dillon, 1963; Lee, 1969; Nied and Batterman, 1972; Raniecki and Sawczuk, 1975; Mroz and Raniecki, 1976; Lehman, 1979). A significant contribution of the work by plastic deformation is converted into heat. The work done by plastic deformation per unit volume can be evaluated by integrating the material stress–strain curve. This internal dissipation term, which constitutes an important part of the nonlinear coupled thermomechanical analysis, is readily detected by infrared thermography. The proposed infrared thermographic technique is mainly concerned with the differences in temperature (or thermal gradients) that exist in the material rather than with the absolute values of temperature. It conveniently detects the *dissipation evolution* of the material under loading. Ignoring the significance of the coupled thermomechanical equation, the attempt by Leaity and Smith (1989) was unsuccessful in monitoring thermoemissions during fatigue crack-propagation tests. The SPATE technique they used was not designed to detect quantitatively the changes in thermoemissions caused by small and slow crack tip advances.

The work, reported in this paper, considers the intrinsic dissipation as the most accurate indicator of damage manifestation. It highlights the advantages of the infrared thermographic technique, used for the detection and the discrimination of physical phenomena involved in this nonlinear coupled thermomechanical effect.

5. Short-time evaluation of fatigue limit

Infrared thermography is a convenient technique for producing heat pictures from the invisible radiant energy emitted from stationary or moving objects at any distance and without surface contact or any perturbation of the actual surface temperature of the objects viewed. The temperature rise ahead of a fatigue crack has been measured and thus proved using an AGA thermovision camera by Attermo and

Östberg (1971). Attempts to measure and characterise the heat generated during the cyclic straining of composite materials have also been made. The scanning infrared camera was used to visualise the surface-temperature field on steel and fiberglass-epoxy composite samples (Charles et al., 1975) during fatigue tests. In this work, all tests are performed with the usual infrared system AGEMA.

5.1. Infrared scanner

A scanning camera, analogous to a television camera, utilises an infrared detector in a sophisticated electronics system. It detects radiated energy and converts it into a detailed real-time thermal picture in a video system either in colour or monochromatically. Response times are shorter than 1 μs. Temperature differences in the heat patterns are discernible instantly and are represented by several hues. The quantity of energy W (W m^{-2} μm^{-1}), emitted as infrared radiation, is a function of the temperature and emissivity of the specimen. The higher the temperature, the more important the emitted energy. Differences of radiated energy correspond to differences of temperature. The AGA 782 SW infrared scanner unit in use comprises:

- a set of infrared lenses which focuses the electromagnetic energy, radiating from the object being scanned, into the vertical prism,
- an electro-optical mechanism which discriminates the field of view in 10^4 pixels by means of two rotating vertical (180 rpm) and horizontal (18,000 rpm) prisms with a scanning rate of 25 fields per second,
- a set of relay optics containing a selectable aperture unit and a filter cassette unit which focuses the output from the horizontal prism onto a single-element point detector, located in the wall of a Dewar chamber,
- a photovoltaic SW short-wave infrared detector composed of Indium Antimonide InSb which produces an electronic signal output varying in proportion to the radiation from the object within the spectral response 3.5 μm to 5.6 μm,
- a liquid nitrogen Dewar which maintains the InSb detector at a temperature of -196°C allowing a very short response time of about one microsecond, and
- an electronic control with preamplifier that produces a video signal on the display screen.

The received radiation has a nonlinear relation with the object temperature, can be affected by atmosphere damping, and includes reflected radiation from the object's surrounding. In consequence, calibration and correction procedures have to be applied. Knowing the temperature of the reference, the view-field temperature can then be calculated with a sensitivity of 0.1°C at 20°C. This infrared device is used to scan the following two fatigue test programs.

5.2. Rotating bending tests

The material for the rotating bending tests was XC55 steel, quite extensively used in automobile construction. To minimise scatter, the 6.74 mm in diameter specimens have been prepared from a single melt. The number of load cycles was 10^7 corresponding to the automobile fatigue damage. Cyclic fatigue tests were performed on a four-point loading rotating bending Schenck machine running at a frequency of 100 Hz. A total of 18 specimens was step-tested according to the Staircase or Up-and-Down method. This procedure means that each specimen was run for 10^7 cycles at 380 MPa for example, whereupon the stress was raised in 10 MPa steps in the absence of failure and the stress was lowered otherwise. Using standard methods of statistical analysis, the fatigue limit has been estimated to be equal to 399 MPa with a standard deviation of 41 MPa (Fig. 1).

A series of five rotating bending tests have been scanned by the infrared system at different stress levels that must be chosen in accordance with the step-by-step procedures for using statistical methods in usual fatigue testing. All specimens were coated with matte spray paint to maximise their emissivity. The paint coating raises the surface emissivity to a uniform high level. In addition, it allows examination of the surface which is undertaken at oblique angles, without degradation of sensitivity. The recommended paint coating will also reduce surface reflections and will ensure uniformity of response across the specimen. With a loading frequency of 100 Hz and after stabilisation of the temperature rise, the load duration chosen was 30 s and 60 s corresponding to 3000 load cycles and 6000 load cycles, respectively.

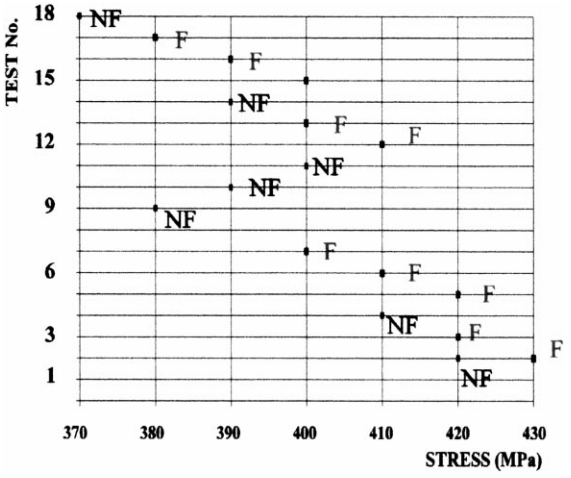

Fig. 1. Standard staircase determination of fatigue limit of XC55 steel.

The AGEMA SW-782 infrared scanner, incorporating a high-temperature filter and equipped with a real-time system DISCON (digital infrared system for colouration) converting thermal images into a ten-colour isotherm display, was used to record the bulk of the heat emission data. That device displays a ten-colour calibrated surface-temperature picture of the specimen. Each colour hue corresponds to 0.2°C.

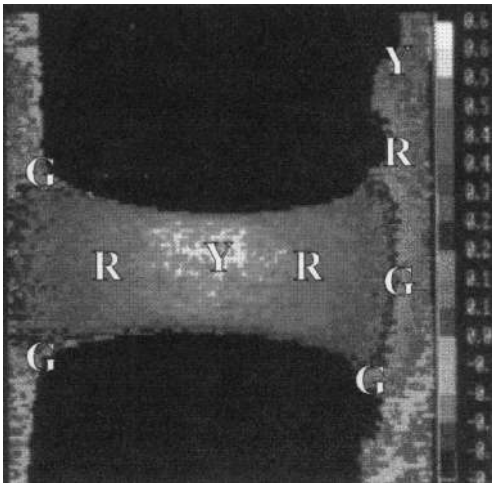

Fig. 2. Intrinsic dissipation of the specimen under 380 MPa after 3000 load cycles (Temperature scale is given in °C).

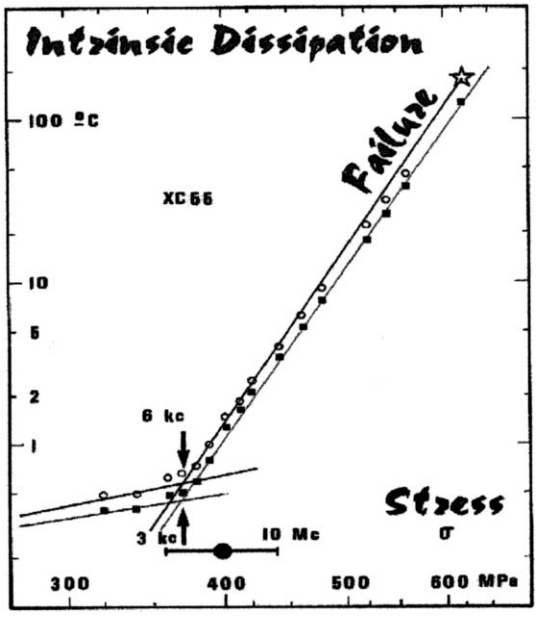

Fig. 3. Graphical determination of fatigue limit of XC55 steel.

A computer-aided thermography software TIC 8000 allowed the data reduction of the thermal images that shows heat generation after 3000 and 6000 load cycles (Fig. 2). These thermal images provided quantitative values of the intrinsic dissipation of a steel specimen in rotating bending caused by 3000 and 6000 load cycles. The same procedure has been applied for each load step.

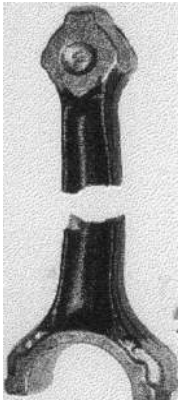

Fig. 4. Connecting rods under tension–compression fatigue tests ($R = +2$).

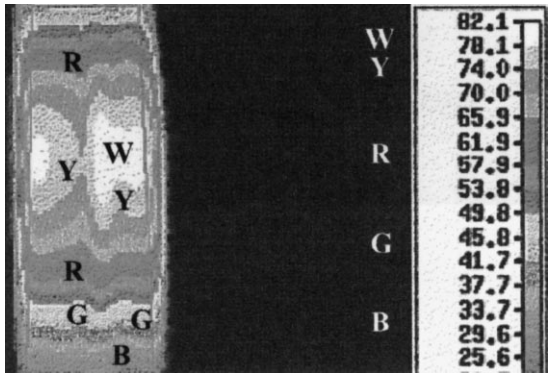

Fig. 5. Intrinsic dissipation of the connecting rod after 2000 load cycles (Temperature scale is given in °C).

The manifestation of the fatigue damage mechanism is revealed by a break of the intrinsic dissipation regime of the loaded specimen. Experimental results have been summarised in Fig. 3 where it can be seen how the fatigue limit is determined using a graphical procedure. The threshold of critical thermal dissipation is roughly the same for the 3000 cycles and 6000 cycles curves, and it corresponds to the value deduced from standard procedure. The star point at coordinates (600 MPa, 180°C) represents the last load step at which failure occurred. These experiments have shown that the infrared thermographic technique can provide the fatigue limit of XC55 steel within a few hours instead of the several months required when using the standard staircase method (Fig. 1). As the results on the cylindrical specimens were successful, this infrared thermographic technique was used to determine the fatigue limit of the connecting rods.

5.3. Tension–compression tests on connecting rods

Five tension–compression tests on connecting rods, prepared from a single melt and subject to a stress ratio $R = \sigma_{max}/\sigma_{min} = -2$, have been scanned by the infrared system at different stress levels in accordance with the step-by-step procedure as specified in Section 5.2. All connecting rod specimens were also coated with matte spray paint to maximise their emissivity (Fig. 4).

The testing procedure was similar to the one for the rotating bending case with cylindrical specimens. With a loading frequency of 20 Hz and after stabilisation of the temperature, the load duration chosen was 100 s corresponding respectively to 2000 load cycles. The thermal images (Fig. 5), processed by TIC 8000, provided quantitative values of the intrinsic dissipation of the connecting rods causing by 2000 load cycles. The same procedure has been applied for each load step.

The same thermal phenomenon as for the previous case of rotating bending was detected. Experimental results have been summarised in Fig. 6 where it can be seen how the fatigue limit is determined using a graphical procedure. The threshold of critical thermal dissipation corresponds to the value deduced from standard procedure. These experiments have shown that infrared thermography can provide the fatigue limit of connecting rods within a few hours

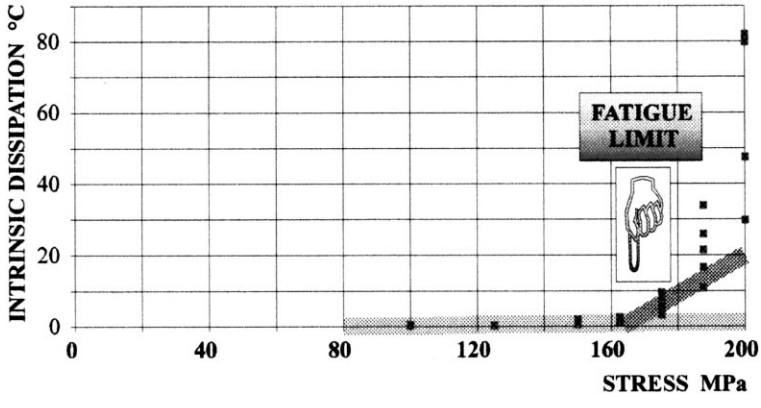

Fig. 6. Graphical determination of fatigue limit of a connecting rod.

instead of several months when using the standard staircase method. Subsequently, several other different fatigue test programs have been performed.

5.4. Fatigue testing on other automotive components and systems

This experimental procedure has been extended with success to the fatigue resistance evaluation of other automotive components and systems: steel cylindrical specimens under cyclic tension–compression (stress ratio $R = -1$), nodular cast iron cylindrical specimens under cyclic torsion loading (stress ratio $R = -1$), cast iron, micro-alloyed, quenched, and tempered steel connecting rods under cyclic tension–compression ($R = -1$), and welded steel tubes under cyclic bending.

6. Concluding remarks

This work has demonstrated that the material dissipativity under fatigue loading is the most sensitive and accurate manifestation of damage. Owing to the thermomechanical coupling, infrared thermography provides a non-destructive real-time test with no contact to observe the physical processes of metal degradation and to detect the occurrence of intrinsic dissipation.

Thus, it readily provides a measure of the material damage and permits evaluation of the sharp limit of a low accumulation of damage beyond which the material leads quickly to failure.

This paper illustrates the use of quantitative infrared thermography as a non-destructive and non-contact technique to detect the manifestation of the physical process of fatigue, and to evaluate rapidly in a few hours the fatigue limit of automotive components. The proposed technique has been applied successfully to metallic materials: different types of steels, cast iron, etc., on diverse stress paths (reversed tension, rotating bending, cyclic torsion, etc.). It consists of detecting the onset of intrinsic dissipation or *damage indicator*, due to the thermomechanical coupling, as the specimen is excited by a fluctuating load. Intrinsic dissipation is thus a scalar parameter which is readily evaluated by infrared thermography. It provides a rapid evaluation of the fatigue strength of connecting rods, traditionally determined by very time-consuming procedures.

References

Allen, D.H., 1985. A prediction of heat generation in a thermoviscoplastic uniaxial bar. Int. J. Solids and Struct. 21 (4), 325–342.

Attermo, R., Östberg, G., 1971. Measurements of the temperature rise ahead a fatigue crack. Int. J. Fract. Mech. 7, 122–124.

Ballard, P., Dang-van, K., Deperrois, A., Papadopoulos, Y.V., 1995. High cycle fatigue and a finite element analysis. Fatigue Fract. Eng. Mater. Struct. 18 (3), 397–411.

Baxter, W.J. (1983), Oxide films: quantitative sensors of metal fatigue. Fatigue mechanisms: Advances in Quantitative Measurement of Physical Damage. ASTM STP 811, 115–136.

Bui, H.D., Ehrlacher, A., Nguyen, Q.S., 1981. Etude expérimentale de la dissipation dans la propagation de la fissure par thermographie infrarouge. C.R. Acad. Sci. 293 (II), 1015–1017.

Bui, H.D., Stolz, C. (1987), Damage theories for brittle and ductile materials. In: Herrmann, Larsson (Eds.), Fract. of Non-Metallic Mater., 33–46.

Cabañas-Moreno, I.G., Yang, M.S., Wertman, J.R., Roth, M., Zhang, Z.Y., Wignall, G.D., Koehler, W.C. (1983), Studies of grain boundary cavitation by small-angle neutron scattering. Fatigue mechanisms: Advances in Quantitative Measurement of Physical Damage. ASTM STP 811, 95–114.

Charles, J.A., Appl, F.J., Francis, J.E., 1975. Using the scanning infrared camera in experimental fatigue studies. Exp. Mech. 14 (4), 133–138.

Dang-van, K. (1973), Sur la résistance à la fatigue des métaux, Sc. et Techn. Armement, Mémorial Artillerie Française, 3e fascicule, 647–722.

Deperrois, A. (1991), Sur le calcul de limite d'endurance des aciers, Thèse de Doctorat de l'Ecole Polytechnique.

Dillon, O.W. Jr., 1963. Coupled thermoplasticity. J. Mech. Phys. Solids 11, 21–23.

Ellyin, F., Kujawski, D., 1984. Plastic strain energy in fatigue failure. Trans. ASME 106, 342–347.

Farren, W.S., Taylor, G.I., 1925. The heat developed during plastic extension of metals. Proc. R. Soc. A 107, 422–428.

Field, J.L., Behnaz, F., Pangborn, R.N. (1983), Characterization of microplasticity developed during fatigue. Fatigue mechanisms: Advances in Quantitative Measurement of Physical Damage. ASTM STP 811, 71–94.

Habib, K., Husain, A., Failure analysis of a broken diesel engine, Fatigue, Butterworth-Heinemann, Vol. 16, July 1994, 357–359.

Irwin, G.R. (1965), Fracture, Encyclopedia of Physics, II, Springer-Verlag, Heidelberg, 7.

James, M.R., Morris, W.L. (1983), The role of microplastic deformation in fatigue crack initiation. Fatigue mechanisms: Advances in Quantitative Measurement of Physical Damage. ASTM STP 811, 46–70.

Kachanov, L.M., 1958. Time of rupture process under creep conditions. Izv. Akad. Nauk. S.S.R. Otd. Tekh. Nauk. 8, 26–31.

Kitagawa, H., Nakasone, Y., Miyashita, S. (1983), Measurement of fatigue damage by randomly distributed small cracks data. Fatigue mechanisms: Advances in Quantitative Measurement of Physical Damage. ASTM STP 811, 233–263.

Kratochvil, J., Dillon, O.W. Jr., 1969. Thermodynamics of elastic–plastic materials as a theory with internal state variables. J. Appl. Phys. 40, 3207–3218.

Lee, E.H., 1969. Elastic plastic deformations at finite strains. J. Appl. Mech. 36, 1–6.

Lehman, Th., 1979. Coupling phenomena in thermoplasticity. SMIRT 5, Berlin, Paper L1/1.

Leaity, G.P., Smith, R.A., 1989. The use of SPATE to measure residual stresses and fatigue crack growth. Fatigue Fract. Eng. Mater. Struct. 12 (4), 271–282.

Loye, C., Bathias, C., Retali, D., Devaux, J.C. (1983), The plastic zone ahead of fatigue crack in 316 stainless steel, fatigue mechanisms: advances in quantitative measurement of physical damage. ASTM STP 811, 427–444.

Luong, M.P., 1990. Infrared thermovision of damage processes in concrete and rock. Eng. Fract. Mech. 35 (1–3), 127–135.

Mann, J.Y. (1983), Aircraft fatigue with particular emphasis on Australian operations and research. In: Proc. 12th ICAF Symp. May 1983 Toulouse. Labourdette, R., Deviller, D. (Eds.), Paper 1.0.

McEvily, A.J. (1983), On the quantitative analysis of fatigue crack propagation. Fatigue mechanisms: Advances in Quantitative Measurement of Physical Damage. ASTM STP 811, 289–312.

McLester, R. (1988), Railway component fatigue testing. In: Full-scale fatigue testing of components and structures. Marsh, K.J. (Ed.), Butterworth, London, 59–76.

Moore, H.F., Kommers, J.B., 1921. Fatigue of metals under repeated stress. Chem. Met. Eng. 25, 1141–1144.

Morrow, J.D. (1965), Cyclic plastic strain energy and fatigue of metals, Internal Friction Damping and Cyclic Plasticity, ASTM STP 378, July, 45–84.

Mroz, Z., 1983. Hardening and degradation rules for metals under monotonic and cyclic loading. J. Eng. Mater. Technol., ASME 105, 113–119.

Mroz, Z. (1986), Phenomenological constitutive models for metals, Modelling small deformations of polycrystals, Elsevier, Amsterdam, 293–344.

Mroz, Z., Raniecki, B., 1976. On the uniqueness problem in coupled thermoplasticity. Int. J. Eng. Sci. 14, 211–221.

Mughrabi, H., Wang, R.H., Differt, K., Essmann, U. (1983), Fatigue crack initiation by cyclic slip irreversibilities in high-cycle fatigue. Fatigue mechanisms: Advances in Quantitative Measurement of Physical Damage. ASTM STP 811, 5–45.

Nied, H.A., Batterman, S.C., 1972. On the thermal feedback reduction of latent energy in the heat conduction equation. Mat. Sci. Eng. 9, 243–245.

Oliver, D.E. 1986. Stress pattern analysis by thermal emission (SPATE). In: Dynamic Stress Analyser. Ometron Limited, UK, Chap. 14, 1-28.

Pluvinage, G.C., Raguet, M.N. (1983), Physical and mechanical measurement of damage in low-cycle fatigue: applications for two-level tests. Fatigue mechanisms: Advances in Quantitative Measurement of Physical Damage. ASTM STP 811, 139–150.

Polak, J., Vasek, A., Obrtlik, K., 1996. Fatigue damage in two step loading of 316L steel: I. Evolution of persistent slip bands —II. Short crack growth. Fatigue Fract. Eng. Mater. Struct. 19 (2/3), 147–163.

Ranganathan, N., Petit, J. (1983), Quantitative measurements in the plastic zone caused by a single overload in air and vacuum. Fatigue mechanisms: Advances in Quantitative Measurement of Physical Damage. ASTM STP 811, 464–484.

Raniecki, B., Sawczuk, A., 1975. Thermal effects in plasticity. Z. Angew. Math. Mech. 55, 333–341 and 363–373.